Coherent photoproduction of vector mesons on deuterium at 5.5 GeV*

V. P. Gupta, S. Y. Fung, Y. T. Oh, R. T. Poe, D. Sager, and B. Shen
Physics Department, University of California, Riverside, California 92502

G. Gidal, R. Ely, R. W. Birge, and C. Scale
Lawrence Berkeley Laboratory, University of California, Berkeley, California 94720
(Received 29 December 1975)

Coherent photoproduction of vector mesons ρ^0, ω, ϕ, and ρ' on deuterium was studied using the SLAC 82-in. bubble chamber exposed to linearly polarized photons at 5.5 GeV. The reaction channel $\gamma d \to \pi^+\pi^- d$ was studied in detail. Nine independent density-matrix parameters have been determined from the ρ^0 decay distribution. ρ production in this channel was found to proceed almost completely through natural-parity exchange for $|t| \leq 0.25$ GeV^2 and conserve s-channel c.m. helicity for $|t| \leq 0.15$ GeV^2. A measurement of differential cross section for this channel has been made.

INTRODUCTION

In this article we report the results of an experimental study of the mechanism of coherent photoproduction of vector mesons on deuterium at 5.5-GeV photon energy. The data come from a study of the following reaction channels:

(a) $\gamma d \to \rho^0 d \to \pi^+\pi^- d$,

(b) $\gamma d \to \omega d \to \pi^+\pi^-\pi^0 d$,

(c) $\gamma d \to \phi d \to k^+k^- d$,

(d) $\gamma d \to \rho' d \to 2\pi^+ 2\pi^- d$.

The experiment was performed using the SLAC 82-in. bubble chamber and the Compton back-scattered laser beam.[1-3] These coherent channels are especially suited for studying the production mechanisms for these mesons as only $I=0$ exchange in the t channel is allowed.

The SLAC facilities with the combined utilization of the back-scattered laser beam and the bubble chamber have the following advantages, not all of which were available in previous studies[4] of coherent vector-meson photoproduction on deuterons: nearly monoenergetic photon spectrum, a highly polarized beam, and a 4π detection efficiency provided by the bubble chamber.

The recent measurements on ρ^0 production have been performed at DESY,[5] Cornell,[6] and SLAC[7] with polarized photons. The SLAC experiments, using bubble-chamber and almost monochromatic photon beams, have resulted in a detailed study of exchange mechanisms involved in the photoproduction reactions on hydrogen. They have observed a lower ρ^0 mass value and shape-skewing.

So far only a few bubble-chamber experiments have been performed [4,8,9] on the coherent photoproduction of resonances in deuterium, and thus much fewer data exist on the γd interactions. In this experiment we have made a detailed photoproduction mechanism study of the ρ^0 meson on deuterium. For other vector-meson productions, the mass distributions are presented. No detailed study was performed due to limited statistics.

I. EXPERIMENTAL PROCEDURE

The deuterium-filled 82-in. bubble chamber was exposed to a nearly monoenergetic linearly polarized photon beam of 5.5 GeV at SLAC. A total of 510 888 pictures were taken in three separate exposures.

All the film was scanned for hadronic events with two or more outgoing charged tracks. The e^+e^- pairs were also counted on two frames in sequence at an interval of 50 frames on each roll of film. The event scans and the pair counts were performed in the same fiducial area. A total of 34 891 events, with two to seven outgoing charged tracks, were found and classified according to topology in Table I. The average number of e^+e^- pair counts was 6.33 pairs per frame.

These events and pairs were measured on the LBL COBWEB data reduction system.[10] The number of events that could not be measured due to secondary scatters or track obscuration consist

TABLE I. Topological events statistics.

Topology	Total scanned events	Unmeasurable events	Poorly measured events	No fits
2-prong	6917	548	106	331
3-prong	16753	1195	1042	1001
4-prong	3661	278	205	340
5-prong	6278	525	548	643
6-prong	579	35	66	88
7-prong	703	56	95	87

of 8% of the total scanned events and are shown in Table I.

The LBL computer program SIOUX (TVGP-SQUAW) was used to reconstruct the events and e^+e^- pairs. Events with an even number of prongs (with an unseen positive track) were fitted assuming the unseen track to be either an impulse proton or a recoil deuteron. In both cases the momentum of the track was taken to be zero, and the errors assigned to the momentum were $\Delta P_x = \Delta P_y = 0.75\Delta P_z = \pm 30$ MeV/c for an invisible proton and $\Delta P_x = \Delta P_y = 0.8\,\Delta P_z = \pm 40$ MeV/c for a missing recoil deuteron. Z is the direction of the optical axis.

The photon energy spectra obtained from the measurement and fitting of e^+e^- pairs are shown in Fig. 1. The top energy spectrum is the combination of the three spectra which are obtained from the three exposures. The spectrum peaks at 5.5 GeV and has a full width at half-maximum (FWHM) of 0.6 GeV. For subsequent analysis of events we exclude the low-energy tail of the photon spectrum, $E_\gamma < 4.7$ GeV, which contains about 18% of the photons. The polarization of the photon beam was calculated, using the formalism of Murray and Klein,[1] to be $(91 \pm 2)\%$.

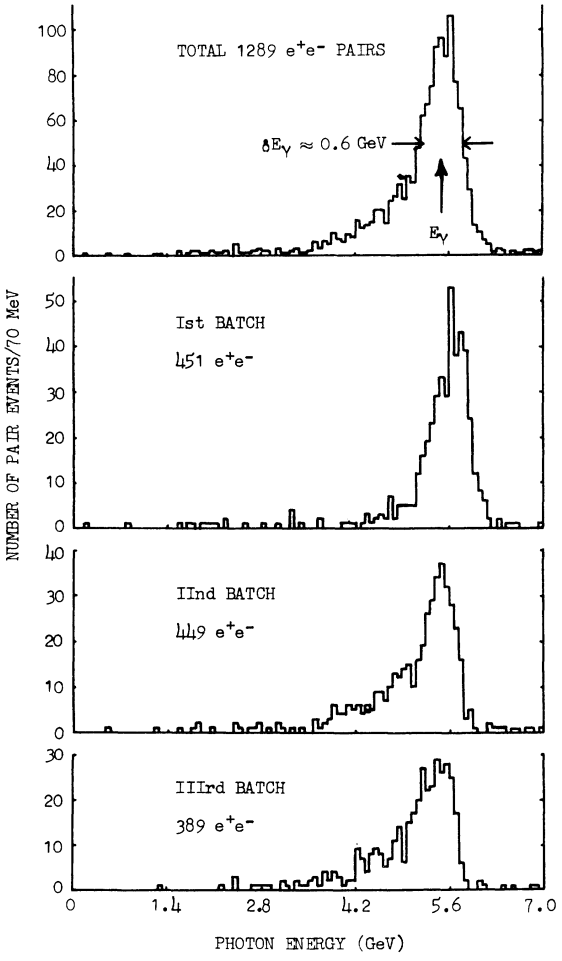

FIG. 1. Photon energy spectra.

In fitting, the beam momentum was treated as unknown, that is, no constraint was placed on the incident photon momentum, whereas the photon beam was assigned a dip of $-0.3°$ and an azimuth angle of 93.1° as determined from the measurements of e^+e^- pairs. Thus hypotheses (a), (c), and (d) have three constraints in the kinematic fitting and hypothesis (b) has zero constraint. All three-constraint fits were required to have kinematic χ^2 less than 26.

Eighty-seven percent of the total scanned events passed the SIOUX processing as shown in Table I. The number of failing events is given in the last two columns of Table I (events under the heading "Poorly measured events" could not pass TVGP, whereas events in the last column could not pass SQUAW). The number of passing events, fitted to various hypotheses for 2–5 outgoing tracks, is given in Table II. These numbers correspond to only those events with fitted photon energy in the range of 4.7–6.2 GeV. However, both unique and ambiguous fits to different hypotheses are included.

II. FITTING PROCEDURE FOR THE REACTION $\gamma d \to \pi^+\pi^- d$

In the kinematic analysis of two- and three-prong events, no constraint was placed on the incident photon momentum and the following final-

TABLE II. Number of events fitted to different hypotheses (not uniquely) for the fitted photon energy within the range 4.7–6.2 GeV.

Hypothesis	Number of constraints	Number of events fitted when visible tracks are 2	4	3	5
$\gamma d \to \pi^- pp$	3	26		18	
$\to \pi^- pp\pi^0$	0	1305		2777	
$\to \pi^-\pi^+ pn$	0	1563		3620	
$\to \pi^-\pi^+ d$	3	702		474	
$\to \pi^-\pi^+ d\pi^0$	0	...		2767	
$\to k^- k^+ d$	3	465		88	
$\to k^- k^+ pn$	0	1724		4046	
$\gamma d \to \pi^-\pi^-\pi^+ pp$	3		374		149
$\to \pi^-\pi^-\pi^+ pp\pi^0$	0		1028		1681
$\to \pi^-\pi^-\pi^+\pi^+ pn$	0		987		1882
$\to \pi^-\pi^-\pi^+\pi^+ d$	3		10		75
$\to \pi^-\pi^-\pi^+\pi^+ d\pi^0$	0		...		1384

state hypotheses were considered:

(i) three-constraint reactions

(a) $\gamma d \to \pi^+ \pi^- d$,

(b) $\gamma d \to \pi^- p p$,

(c) $\gamma d \to K^+ K^- d$;

(ii) zero-constraint reactions

(d) $\gamma d \to \pi^+ \pi^- p n$,

(e) $\gamma d \to \pi^- \pi^0 p p$,

(f) $\gamma d \to \pi^+ \pi^- \pi^0 d$,

(g) $\gamma d \to K^+ K^- p n$.

From the 16 753 (6917) scanned events we found 365 (603) three- (two-) prong events which gave 3C fits to the reaction

$$\gamma d \to \pi^+ \pi^- d \qquad (1)$$

with fitted photon energy, E_γ, in the interval $4.7 \leq E_\gamma \leq 6.2$ GeV and $\chi^2 \leq 15$. Owing to the low binding energy of the deuteron, coherent deuteron reactions are characterized by a steeply decreasing momentum-transfer distribution. Since deuterons with $P<110$ MeV/c are undetected on the film, a large fraction of the coherent events will thus have an invisible deuteron (two-prong topology). These events will generally also pass the corresponding 0C fit with an outgoing proton and neutron ($\gamma d \to \pi^+ \pi^- p_s n$). However, if the event is really a coherent one, the fitted proton and neutron both will be moving nearly in the same direction and their invariant mass will be enhanced in the region of the deuteron mass. By inspecting, therefore, the final state $\gamma d \to \pi^+ \pi^- p_s n$ fits and requiring $M(p_s n) \leq 1.885$ GeV we expect the two-prong sample to be free of background.

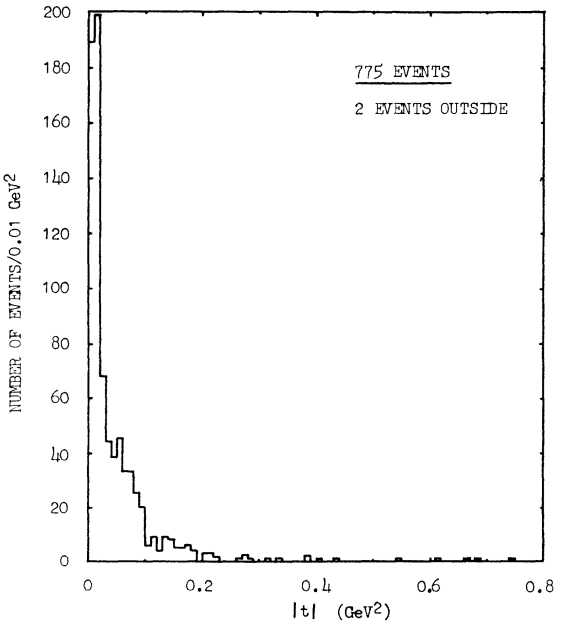

FIG. 2. t distribution for the events accepted for ρ^0 study.

For our ρ^0 study we accepted only those two-prong events which had $|t_{\min}| = 0.003 \leq |t| \leq 0.025$ GeV^2 and which also fitted to the hypothesis $\gamma d \to \pi^+ \pi^- p_s n$ with $M(p_s n) \leq 1.885$ GeV, and those three-prong events which had $|t| > 0.025$ GeV^2. Here t is the square of the four-momentum transfer from the incoming photon to the dipion mass. In this reaction the minimum momentum transfer is 0.003 GeV^2, and $|t| > 0.025$ GeV^2 corresponds to deuteron track lengths of greater than 2 mm in the bubble chamber, and nearly all are three-prong events with a measured d track. The t distribution for the sample of 775 events thus obtained is shown in Fig. 2. The coherent ρ^0 production forward peak is clearly seen.

A. Mass distributions

Figure 3 shown the $\pi^+\pi^-$ effective-mass distributions for reaction (1). The top spectrum is

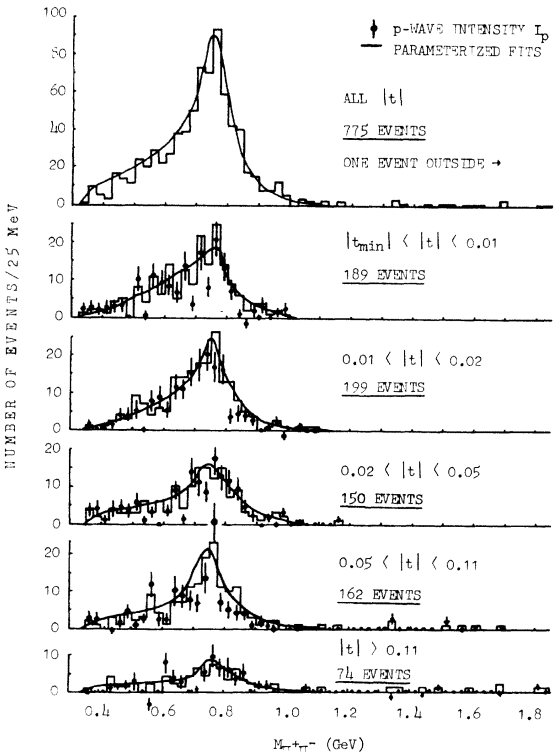

FIG. 3. $\pi^+\pi^-$ mass distribution for different t intervals. The helicity-conserving p-wave intensity I_p is shown by the points ϕ. The curves give the results of maximum-likelihood fits to the channel using the parameterization method.

for all the events; below, these distributions are repeated for events grouped into various t intervals. The ρ^0 production is observed in these $\pi^+\pi^-$ mass distributions. It is clear from Fig. 3 that the ρ^0 enhancement does not have the shape of a p-wave Breit-Wigner distribution,[11,12] and changes shape as a function of t.[7]

In Fig. 4 we have shown the $\pi^{\pm}d$ effective-mass distributions to study the production of d^*. The πd mass distributions, however, show no d^* enhancement near $M(\pi d) = 2.2$ GeV as reported in some πd and Kd experiments.[13]

B. Parametrization

Hilpert *et al.*,[4] in the reaction $\gamma d \to \pi^+\pi^- d$, obtained reasonable fits to the $\pi^+\pi^-$ mass distributions. They multiplied the Briet-Wigner distribution with an energy-dependent width (according to Jackson[14]) for the ρ^0 by a mass-skewing factor $(M/M_{\pi\pi})^4$ from the diffraction dissociation model of Ross and Stodolsky.[15] However, in a study[7] of reaction $\gamma p \to \pi^+\pi^- p$ it has been concluded that the ρ^0 Breit-Wigner distribution should be multiplied by $(M/M_{\pi\pi})^{n(t)}$; the parameter $n(t)$ is greater than 5 near $t = 0$ but drops to zero around $-t = 0.5$ GeV^2. In the absence of any precise theory of the line shape of a broad resonance such as the ρ^0, we made maximum-likelihood fits to the events of reaction (1) assuming the density distribution of events is

$$dP = [a_\rho BW_\rho(M_{\pi\pi}) W(\cos\theta_H)(M_0/M_{\pi\pi})^{n(t)} e^{A_\rho t} + a_{PS}] \times d(PS), \tag{2}$$

where

$$BW_\rho(M) = \frac{M}{q(M)} \frac{M_0\Gamma}{(M^2 - M_0^2)^2 + M_0^2\Gamma^2},$$

$$\Gamma = \Gamma_0 \left(\frac{q(M_{\pi\pi})}{q(M_0)}\right)^3 \frac{f(M_{\pi\pi})}{f(M_0)},$$

$$f(M) = [q^2(M) + q^2(M_0)]^{-1},$$

a_ρ, a_{PS} = fraction of ρ^0 production and phase-space background (apart from suitable normalization factors),

$q(M)$ = three-momentum of the pion in the $\pi^+\pi^-$ rest system,

$W(\cos\theta_H) = \frac{3}{4}\sin^2\theta_H$ describes the experimentally observed ρ^0 decay angular distribution in the helicity frame,

$M_0, \Gamma_0, n(t), A_\rho$ = parameters of the fit.

C. Fitting procedure

Computer program OPTIME[16] was used for fitting the data. We first determined M_0, Γ_0, $n(t)$, and A_ρ from an overall fit in the region $-t < 0.11$ GeV^2. With M_0, Γ_0, and A_ρ fixed at these values, the quantities a_ρ, a_{PS} and the final value of $n(t)$ were fitted for different t intervals (see Table III). The fits described the $\pi^+\pi^-$ mass spectra well, as shown by the curves in Fig. 3. The fitted values of $n(t)$ are shown in Fig. 5. Over the accessible t range in this experiment the value of $n(t)$ is in agreement with the findings of the previous study.[7]

In Fig. 6 we display the curves corresponding to $n(t) = 4$ and the best fitted value of $n(t) = 4.93$ for the region $-t < 0.11$ GeV^2. The solid line gives the fit result of $n(t) = 4.93$ with confidence level $\approx 25\%$. The dashed line represents the calculated $\pi^+\pi^-$ distribution with the parameter $n(t)$ set to 4. The confidence level for the latter is less than 0.1%.

In the lowest four t bins (t_{min}–0.11 GeV^2), which

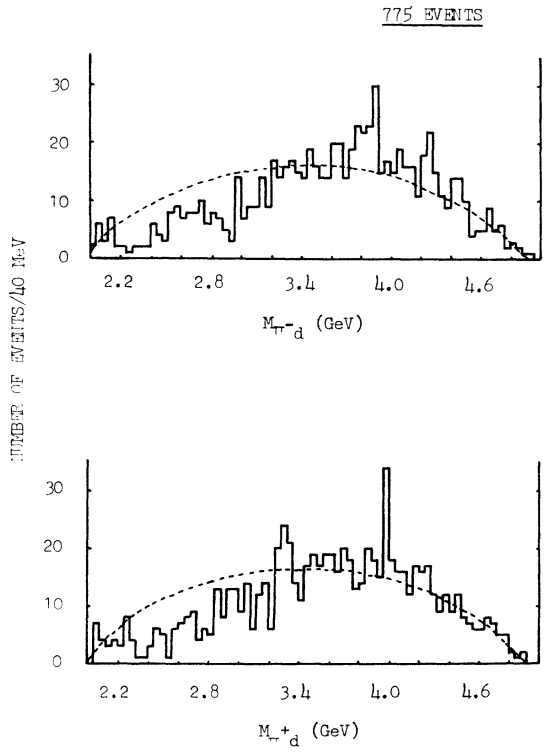

FIG. 4. π^-d and π^+d mass distributions. The final-state three-particle phase space is shown as the dashed curve.

TABLE III. Values of $n(t)$ and event distribution at different t intervals.

$\lvert t\rvert$ (GeV^2)	$n(t)$	Number of events under ρ peak	Phase space
t_{min}–0.01	3.6 ± 1.1	95.6 ± 15.6	93.4 ± 16.0
0.01–0.02	4.7 ± 0.5	183.6 ± 16.9	15.8 ± 7.0
0.02–0.05	5.5 ± 0.4	145.6 ± 15.0	4.4 ± 4.6
0.05–0.11	4.5 ± 0.6	150.2 ± 14.0	11.8 ± 4.7

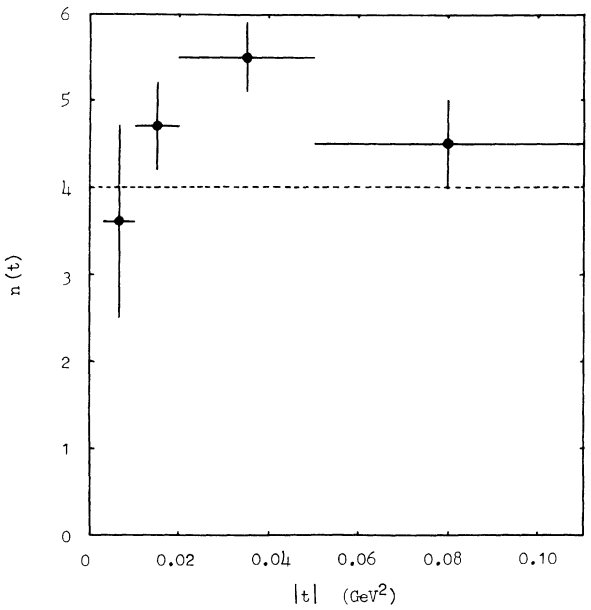

FIG. 5. Fitted values of $n(t)$ as the function of t.

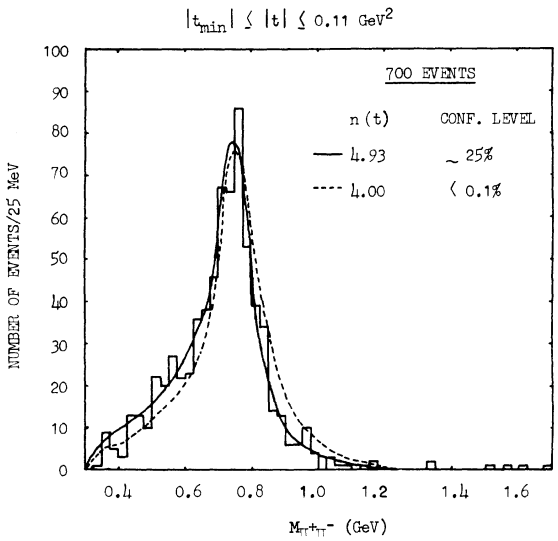

FIG. 6. Results of maximum-likelihood fits using Eq. (2) with $n(t) = 4$ and the optimum value $n(t) = 4.93$.

contain about 90% of the accepted events of reaction (1), we obtained from the fit for the ρ mass and width the values (766 ±5) and (139 ±11) MeV, respectively. The value obtained for the exponential slope, A_ρ, was (35.1 ±1.6) GeV^{-2}.

III. COHERENT ρ^0 PHOTOPRODUCTION ON DEUTERIUM

In this section we discuss the angular distribution of $\pi^+\pi^-$ in their rest system. It will be shown below that the $\pi^+\pi^-$ pairs are in a predominantly p-wave state, so for brevity we refer to them as ρ^0.

A. Analysis of dipion angular-momentum states

The full description of vector-meson photoproduction requires 12 complex amplitudes, or 23 real numbers at a given energy and momentum transfer. With the polarized beam and using the full decay angular distribution of the vector meson it is possible to measure 10 (nine parameters of decay spin-density matrix and the diffraction cross section) of the 23 parameters, whereas only four of these parameters can be determined with unpolarized beams.

We use the formalism of Schilling *et al.*[17,18] for the analysis of the ρ^0 decay angular distribution produced by linearly polarized photons. The results are presented in three frames, namely, helicity (H), Gottfried-Jackson (GJ), and Adair (A) frames. The three frames differ in the choice of the Z axis, the spin-quantization axis. The helicity frame has its Z axis in the direction of the ρ^0 in the overall (γd) c.m. system, the Adair frame in the direction of the incident photon in the overall c.m. system, and the GJ frame in the direction of the incident photon in the ρ^0 rest system. In all these systems the Y axis is taken as the normal to the production plane. For forward-produced ρ^0 mesons, all three systems coincide.

In all three systems the decay angular distribution for ρ^0 can be expressed in terms of nine independent and measureable density-matrix parameters $\rho^\alpha_{\lambda\lambda}$ (see Ref. 19, Appendix A). Let Φ be the angle between the photon polarization vector, $\vec{\epsilon}_\gamma$, and the production plane, and θ and ϕ be the polar and azimuthal angles of the vector $\vec{\epsilon}_{\pi^+}$ in the ρ^0 rest system. Then, for the degree of linear polarization of the photon to be P_γ, the ρ-meson decay angular distribution is given as[18]

$$W(\cos\theta, \phi, \Phi) = \frac{3}{4\pi}\left[\tfrac{1}{2}(1-\rho^0_{00}) + \tfrac{1}{2}(3\rho^0_{00}-1)\cos^2\theta - \sqrt{2}\,\mathrm{Re}\rho^0_{10}\sin 2\theta\cos\phi - \rho^0_{1-1}\sin^2\theta\cos 2\phi\right.$$
$$- P_\gamma\cos 2\Phi(\rho^1_{00}\cos^2\theta + \rho^1_{11}\sin^2\theta - \sqrt{2}\,\mathrm{Re}\rho^1_{10}\sin 2\theta\cos\phi - \rho^1_{1-1}\sin^2\theta\cos 2\phi)$$
$$\left. - P_\gamma\sin 2\Phi(\sqrt{2}\,\mathrm{Im}\rho^2_{10}\sin 2\theta\sin\phi + \mathrm{Im}\rho^2_{1-1}\sin^2\theta\sin 2\phi)\right]. \quad (3)$$

Here $\rho^0_{\lambda\lambda}$ are the density-matrix elements for the unpolarized photons, whereas $\rho^1_{\lambda\lambda}$ and $\rho^2_{\lambda\lambda}$ are due to the photon's linear polarization.

Let $\Psi(=\phi-\Phi)$ be the angle between the $\vec{\epsilon}_\gamma$ and the projection of $\vec{\epsilon}_{\pi^+}$ onto a plane perpendicular to the direction of the incident photon. Then for ρ^0 photoproduction in the near forward direction, the ρ^0 decay distribution in the helicity frame is[7]

$$W(\theta,\Psi)=\frac{3}{8\pi}\sin^2\theta_H(1+P_\gamma\cos2\Psi_H). \quad (4)$$

The decay angular distribution of the $\pi^+\pi^-$ system for events in the ρ mass region, $0.6\leq M_{2\pi}\leq 0.85$ GeV, and for the small momentum transfer, $|t|\leq 0.15$ GeV^2, from this experiment are shown in Fig. 7. The $\cos\theta_H$ distribution is compatible with $\sin^2\theta_H$, consistent with complete helicity conservation at the γ_ρ vertex. The Ψ_H distribution data also show an excellent agreement with the $(1+P_\gamma\cos2\Psi_H)$ curve ensuring that the ρ^0 is almost completely linearly polarized. There is overwhelming evidence for natural J^P exchange in ρ^0 production in our experiment. The scatter plot of Ψ_H vs $\cos\theta_H$ is proportional to $\sin^2\theta_H x(1+P_\gamma\cos2\Psi_H)$ and there is no evidence of any correlation between Ψ_H and $\cos\theta_H$.

In Fig. 8 we present the moment sums, $\sum \mathrm{Re}Y_1^m(\theta,\Psi)$, of the $\pi^+\pi^-$ system in the helicity frame as a function of the $\pi^+\pi^-$ mass for $-t\leq 0.15$ GeV^2. There are strong Y_2^0 and Y_2^2 moments present in the ρ^0 region which follow the asymmetric shape. The Y_2^0 moment shows the behavior expected for the $\sin^2\theta$ decay of ρ^0. No significant

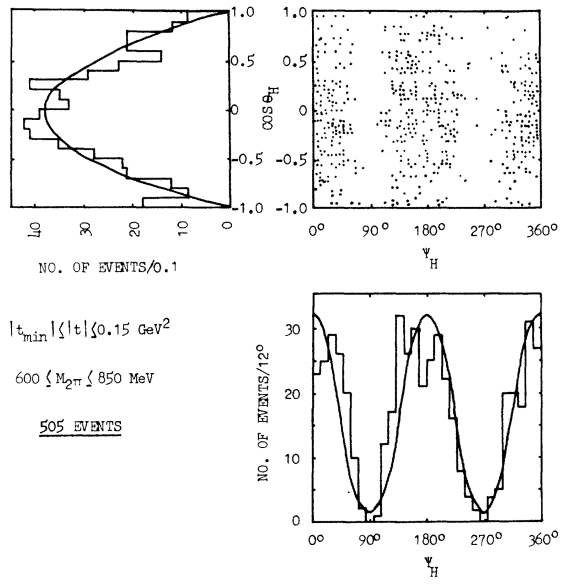

FIG. 7. ρ decay angular distribution in the helicity frame for $|t_{min}|\leq|t|\leq 0.15$ GeV^2 and $0.6\leq M_{2\pi}\leq 0.85$ GeV.

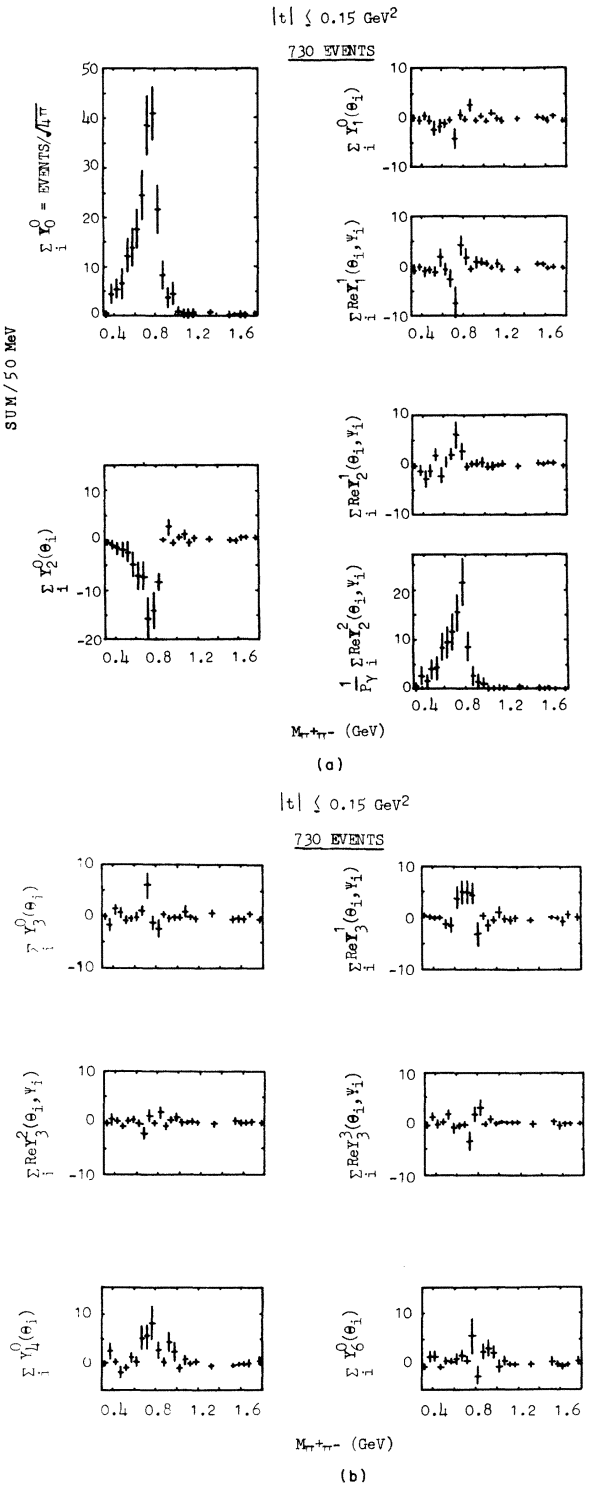

FIG. 8. (a) The dipion moments Y_0^0, $Y_1^0(\theta)$, $Y_1^1(\theta,\Psi)$, $Y_2^0(\theta)$, $Y_2^1(\theta,\Psi)$, and $Y_2^2(\theta,\Psi)$ in the helicity frame as a function of $M_{2\pi}$ for $|t_{min}|\leq|t|\leq 0.15$ GeV^2. (b) The dipion moments $Y_3^0(\theta)$, $Y_1^3(\theta,\Psi)$, $Y_3^2(\theta,\Psi)$, $Y_3^3(\theta,\Psi)$, $Y_4^0(\theta)$, and $Y_6^0(\theta)$ in the helicity frame as a function of $M_{2\pi}$ for $|t_{min}|\leq|t|\leq 0.15$ GeV^2.

moments, other than those associated with a p-wave system, exist in the ρ^0 region indicating a negligible incoherent background in the ρ^0 region.

B. Density-matrix elements of the ρ^0 states

If s-channel helicity were conserved in ρ^0 photoproduction on deuterium, all $\rho^{\alpha}_{\lambda\lambda}$, would be zero except

$$\rho^1_{1-1} = -\mathrm{Im}\rho^2_{1-1} = \tfrac{1}{2}. \tag{5}$$

Our results for nine independent density-matrix elements in Eq. (3), determined by moment analysis[20] (see Ref. 19, Appendix B), are given in Table IV and Fig. 9. Within errors, up to $-t \approx 0.25$ GeV^2, these results clearly show that in the helicity frame the contributions from helicity flip are consistent with zero value and ρ^0 does retain the photon polarization.

For completeness we notice that zero flip in the GJ frame would imply no spin exchange in the t

TABLE IV. ρ density-matrix elements for the reaction $\gamma d \to \rho^0 d$.

$\lvert t\rvert$ (GeV^2)	$t_{\min}$ −0.02	0.02–0.04	0.04–0.08	0.08–0.12	0.12–0.25
			(a) Helicity frame		
ρ^0_{00}	0.138 ± 0.038	0.068 ± 0.058	0.074 ± 0.052	0.128 ± 0.082	0.054 ± 0.082
$\mathrm{Re}\rho^0_{10}$	0.036 ± 0.020	−0.033 ± 0.039	−0.048 ± 0.036	0.058 ± 0.056	0.030 ± 0.058
ρ^0_{1-1}	−0.011 ± 0.036	−0.001 ± 0.065	−0.056 ± 0.058	−0.022 ± 0.092	0.155 ± 0.101
ρ^1_{00}	−0.059 ± 0.060	0.070 ± 0.094	−0.166 ± 0.074	0.140 ± 0.149	−0.115 ± 0.108
ρ^1_{11}	0.115 ± 0.046	0.054 ± 0.084	0.068 ± 0.066	−0.086 ± 0.107	−0.016 ± 0.128
$\mathrm{Re}\rho^1_{10}$	−0.023 ± 0.030	0.038 ± 0.058	0.030 ± 0.057	0.006 ± 0.085	−0.119 ± 0.094
ρ^1_{1-1}	0.428 ± 0.052	0.454 ± 0.089	0.372 ± 0.076	0.477 ± 0.135	0.395 ± 0.156
$\mathrm{Im}\rho^2_{10}$	0.019 ± 0.031	−0.125 ± 0.063	0.040 ± 0.052	0.140 ± 0.079	−0.013 ± 0.090
$\mathrm{Im}\rho^2_{1-1}$	−0.399 ± 0.051	−0.478 ± 0.095	−0.449 ± 0.086	−0.521 ± 0.127	−0.273 ± 0.138
			(b) Gottfried-Jackson frame		
ρ^0_{00}	0.189 ± 0.039	0.129 ± 0.061	0.204 ± 0.057	0.405 ± 0.097	0.316 ± 0.105
$\mathrm{Re}\rho^0_{10}$	0.095 ± 0.021	0.110 ± 0.039	0.171 ± 0.033	0.134 ± 0.053	0.077 ± 0.054
ρ^0_{1-1}	0.014 ± 0.035	0.029 ± 0.063	0.009 ± 0.056	0.116 ± 0.083	0.286 ± 0.087
ρ^1_{00}	−0.098 ± 0.060	0.013 ± 0.097	−0.168 ± 0.092	−0.224 ± 0.165	−0.483 ± 0.172
ρ^1_{11}	0.134 ± 0.044	0.082 ± 0.078	0.070 ± 0.067	0.096 ± 0.100	0.168 ± 0.116
$\mathrm{Re}\rho^1_{10}$	−0.058 ± 0.063	−0.117 ± 0.063	−0.062 ± 0.047	−0.247 ± 0.081	−0.138 ± 0.078
ρ^1_{1-1}	0.408 ± 0.050	0.426 ± 0.084	0.371 ± 0.078	0.296 ± 0.136	0.211 ± 0.154
$\mathrm{Im}\rho^2_{10}$	0.091 ± 0.030	0.056 ± 0.064	0.235 ± 0.056	0.342 ± 0.090	0.174 ± 0.099
$\mathrm{Im}\rho^2_{1-1}$	−0.375 ± 0.051	−0.498 ± 0.094	−0.308 ± 0.082	−0.189 ± 0.116	−0.157 ± 0.126
			(c) Adair frame		
ρ^0_{00}	0.143 ± 0.038	0.063 ± 0.058	0.063 ± 0.052	0.161 ± 0.084	0.079 ± 0.081
$\mathrm{Re}\rho^0_{10}$	0.047 ± 0.020	−0.011 ± 0.039	−0.009 ± 0.035	0.092 ± 0.054	0.071 ± 0.058
ρ^0_{1-1}	−0.009 ± 0.036	−0.004 ± 0.065	−0.061 ± 0.059	−0.006 ± 0.093	0.167 ± 0.101
ρ^1_{00}	−0.063 ± 0.060	0.075 ± 0.095	−0.156 ± 0.073	0.127 ± 0.153	−0.184 ± 0.108
ρ^1_{11}	0.117 ± 0.045	0.051 ± 0.084	0.063 ± 0.067	−0.080 ± 0.106	0.018 ± 0.123
$\mathrm{Re}\rho^1_{10}$	−0.030 ± 0.030	0.009 ± 0.057	0.019 ± 0.057	−0.066 ± 0.083	−0.150 ± 0.098
ρ^1_{1-1}	0.426 ± 0.051	0.457 ± 0.088	0.377 ± 0.076	0.471 ± 0.137	0.361 ± 0.155
$\mathrm{Im}\rho^2_{10}$	0.030 ± 0.030	−0.097 ± 0.063	0.076 ± 0.052	0.194 ± 0.082	0.025 ± 0.092
$\mathrm{Im}\rho^2_{1-1}$	−0.396 ± 0.095	−0.490 ± 0.095	−0.438 ± 0.086	−0.486 ± 0.124	−0.272 ± 0.135

channel, while zero flip in the Adair frame would hold if spin direction was conserved.[21] Since the matrix elements vary significantly with t in the GJ frame, this possibility is ruled out. The most concise way to demonstrate the apparent conservation of helicity in ρ^0 photoproduction is presented in Fig. 10. Consider a frame in the rest system of the ρ^0, in which the ρ^0 density matrix most closely resembles that of the initial photon. Then let β be the angle of rotation around the normal to the production plane that transforms the s-channel helicity frame into this new frame. One actually

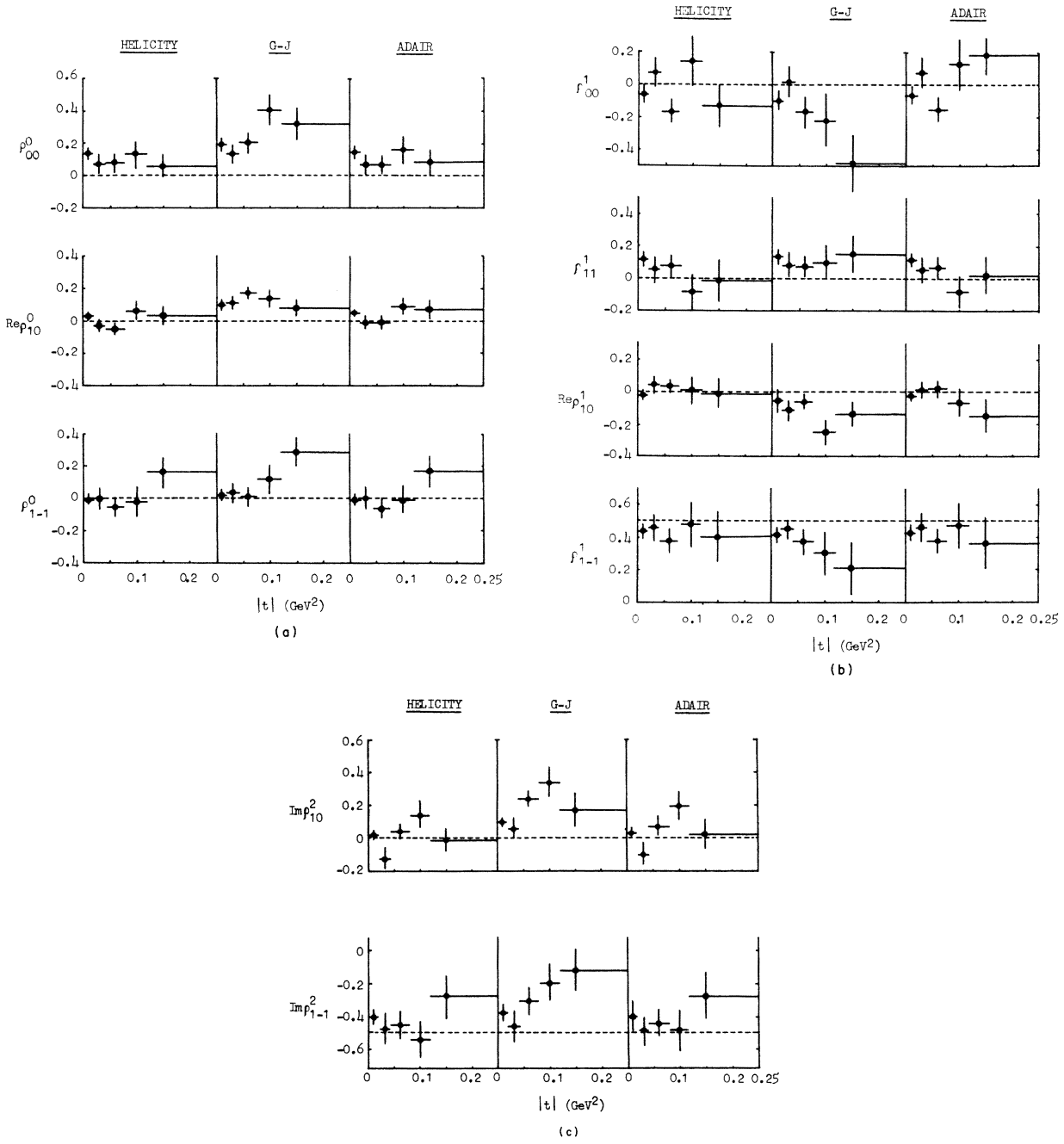

FIG. 9. (a) The spin-density-matrix parameters ρ^0_{00}, $\mathrm{Re}\rho^0_{10}$, and ρ^0_{1-1} as a function of t in the helicity, GJ, and Adair frames. (b) The spin-density-matrix parameters ρ^1_{00}, ρ^1_{11}, $\mathrm{Re}\rho^1_{10}$, and ρ^1_{1-1} as a function of t in the helicity, GJ, and Adair frames. (c) The spin-density-matrix parameters $\mathrm{Im}\rho^2_{10}$ and $\mathrm{Im}\rho^2_{1-1}$ as a function of t in the helicity, GJ, and Adair frames.

minimizes[7]

$$\chi^2(\beta) = \sum_{\lambda,\lambda'\alpha} \left| \frac{\rho^{\alpha}_{\lambda\lambda'}(\beta) - \rho^{\alpha}_{\lambda\lambda'}(\text{photon})}{\delta\rho^{\alpha}_{\lambda\lambda'}(\beta)} \right|^2 , \tag{6}$$

where $\rho^{\alpha}_{\lambda\lambda'}(\text{photon})$ is the ρ^0 density matrix of photon [Eq. (5)]. It is seen in Fig. 10 that β is not far from zero up to $-t = 0.25$ GeV^2. Also shown in this figure are the angles of rotations from the helicity frame into the Adiar frame (curve A), and into the Gottfried-Jackson frame (curve GJ). For $|t| \leq 0.25$ GeV^2, the helicity frame is definitely preferred.

C. ρ production properties

It has been shown that to leading order in energy,[22,23] the overall production cross section, σ, may be split into noninterfering contributions σ^N, σ^U from natural- and unnatural-parity exchanges in the t channel. One could draw stronger conclusions from the density-matrix elements by estimating quantitatively the contributions of σ^N and σ^U to the cross section. The "parity asymmetry" parameter is defined as

$$P_\sigma = \frac{\sigma^N - \sigma^U}{\sigma^N + \sigma^U} .$$

At high energies

$$P_\sigma = 2\rho^1_{1-1} - \rho^1_{00} . \tag{7}$$

Also the "asymmetry ratio" is given as

$$\Sigma = \frac{\sigma_\parallel - \sigma_\perp}{\sigma_\parallel + \sigma_\perp} = \frac{\rho^1_{11} + \rho^1_{1-1}}{\rho^0_{11} + \rho^0_{1-1}} , \tag{8}$$

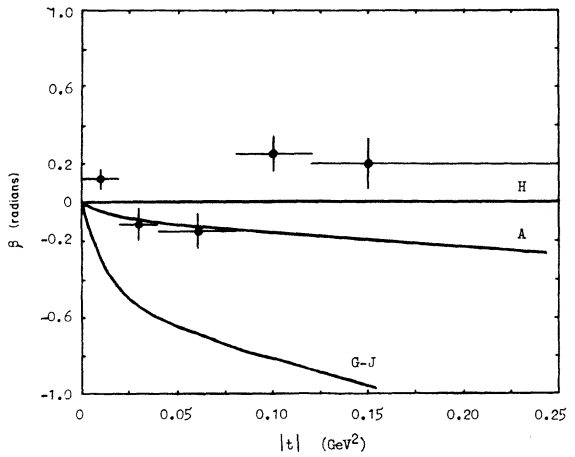

FIG. 10. The angle β for rotation, about the production normal, of the ρ^0 density matrix from the helicity frame in the "minimum flip" system as a function of t. The curves marked H, A, and GJ show where the data would lie if the minimum flip system were the helicity, Adair, and Gottfried-Jackson frames, respectively.

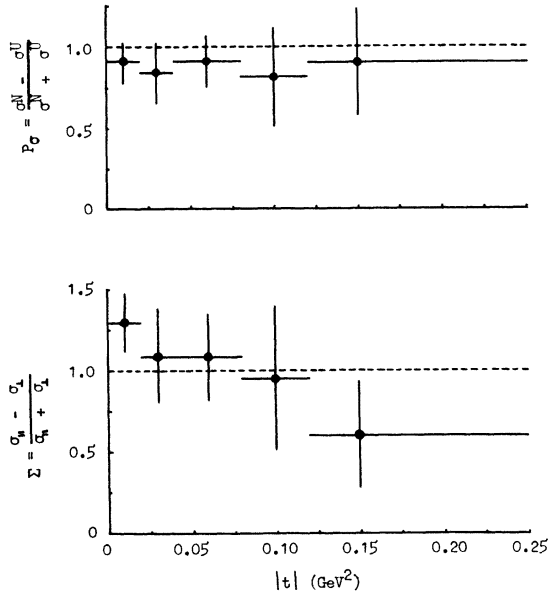

FIG. 11. P_σ and Σ as a function of t.

where $\sigma_\parallel$ ($\sigma_\perp$) is the cross section for the case when the ρ^0 polarization $\vec{\epsilon}_{\pi^+}$ is orthogonal to the production plane and the $\vec{\epsilon}_\gamma$ is parallel (perpendicular) to $\vec{\epsilon}_{\pi^+}$.

In Table V and Fig. 11 we display the quantities P_σ and Σ. We found the contribution from the unnatural-parity exchanges to be $(5.3 \pm 4.5)\%$ and the value of Σ as 1.1 ± 0.2 for the averages over the momentum transfer ranges of $t_{\min}$–0.25 GeV^2.

To see whether the p-wave $\pi^+\pi^-$ system produced by natural exchanges and with helicity conservation is also seen outside the ρ^0 mass region, we have plotted in Fig. 12 ρ^0_{00} and ρ^1_{1-1} in the helicity frame, and P_σ as a function of the $\pi^+\pi^-$ mass. In the ρ^0 mass region $\rho^0_{00} \approx 0$, $\rho^1_{1-1} \approx \frac{1}{2}$, and $P_\sigma \approx 1$, but outside of the ρ^0 mass region these quantities change drastically. This is clear evidence for a background behaving quite differently from the ρ^0.

D. s-channel helicity-conserving p-wave intensity

In order to determine directly the amount of p-wave dipion production in the ρ^0 mass region, we

TABLE V. P_σ and Σ for the reaction $\gamma d \to \rho^0 d$.

$\lvert t \rvert$ (GeV^2)	$P_\sigma = \frac{\sigma^N - \sigma^U}{\sigma^N + \sigma^U}$	$\Sigma = \frac{\sigma_\parallel - \sigma_\perp}{\sigma_\parallel + \sigma_\perp}$
$t_{\min}$–0.02	0.915 ± 0.119	1.293 ± 0.185
0.02–0.04	0.838 ± 0.201	1.093 ± 0.286
0.04–0.08	0.910 ± 0.168	1.082 ± 0.273
0.08–0.12	0.815 ± 0.308	0.947 ± 0.447
0.12–0.25	0.905 ± 0.330	0.603 ± 0.328

make use of the result of Sec. III B that the production mechanism for p-wave $\pi^+\pi^-$ pairs conserves s-channel helicity at the $\gamma\pi^+\pi^-$ vertex for $|t| \leq 0.25$ GeV^2, and so yields pion pairs in a well-defined spin state. This implies that the decay angular distribution for p-wave $\pi^+\pi^-$ pairs is given by Eq. (4), which may be expressed in terms of moments as

$$W(\theta,\Psi) = \frac{1}{\sqrt{4\pi}} Y_{00}^0(\theta) - \frac{1}{\sqrt{20\pi}} Y_2^0(\theta) + 2P_\gamma \left(\frac{3}{40\pi}\right)^{1/2} \mathrm{Re}Y_2^2(\theta,\Psi).$$

In this equation $\mathrm{Re}Y_2^2(\theta,\Psi)$ is least affected by the background due to its Ψ dependence and is used, therefore, to determine the s-channel c.m.s. helicity-conserving p-wave $\pi^+\pi^-$ intensity, I_p, defined as[7]

$$I_p = \frac{\sum_i \mathrm{Re}Y_2^2(\theta_i,\psi_i)}{\langle \mathrm{Re}\, Y_2^2(\theta_i,\psi_i)\rangle} = \frac{\sum_i \mathrm{Re}Y_2^2(\theta_i,\psi_i)}{\int\int d\psi\, d(\cos\theta) W(\theta,\psi)\mathrm{Re}Y_2^2(\theta,\psi)}.$$

After carrying out the integration, we get

$$I_p = \frac{1}{P_\gamma}\left(\frac{40\pi}{3}\right)^{1/2} \sum_i \mathrm{Re}Y_2^2(\theta_i,\psi_i) = \frac{2.5}{P_\gamma}\sum_i \sin^2\theta_i \cos 2\psi_i . \quad (9)$$

Here the summation is over all events. Figure 13 shows the distribution of I_p as a function of t. For $-t \approx 0.1$ GeV^2, the slope of the t distribution and the slope obtained for I_p agree within errors.

In Fig. 3 the dots marked on the histograms show the I_p as a function of $\pi^+\pi^-$ for different t intervals. We notice that the I_p accounts for almost all the events within errors and shows the same skewing (characteristic downward ρ mass shift in photoproduction) as the mass distributions.

IV. CROSS-SECTION DETERMINATION

The electron pairs, since they are the principal background, provide a means to calculate the cross section with very little bias. The photoproduction cross section for hadronic events is obtained by relating the number of hadronic events, N_H, to the number of e^+e^- pairs, N_p, obtained in the same scanning volume, using the known[24] cross section, σ_p, for e^+e^- pair production:

$$\sigma_H = \frac{N_H}{N_P}\sigma_P. \quad (10)$$

Corrections for scanning losses were applied. The losses of two-prong events were mainly due

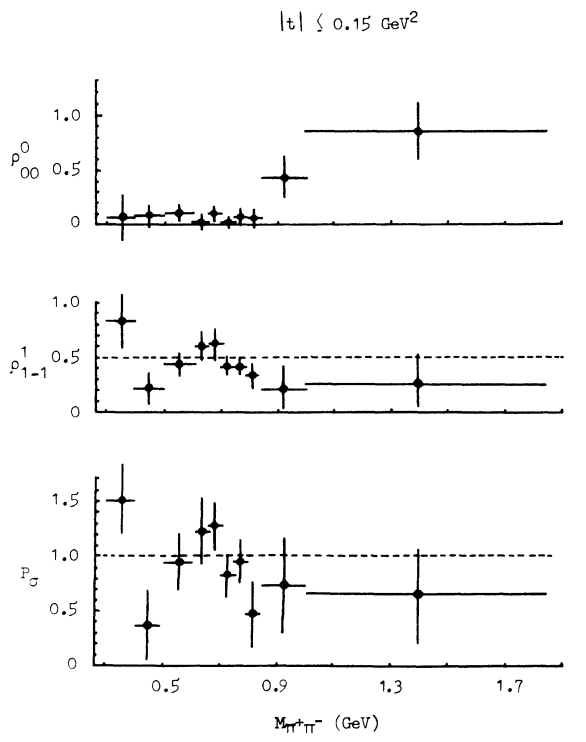

FIG. 12. The density-matrix elements ρ^0_{00} and ρ^1_{1-1} in the helicity frame, and P_σ as a function of $M_{2\pi}$.

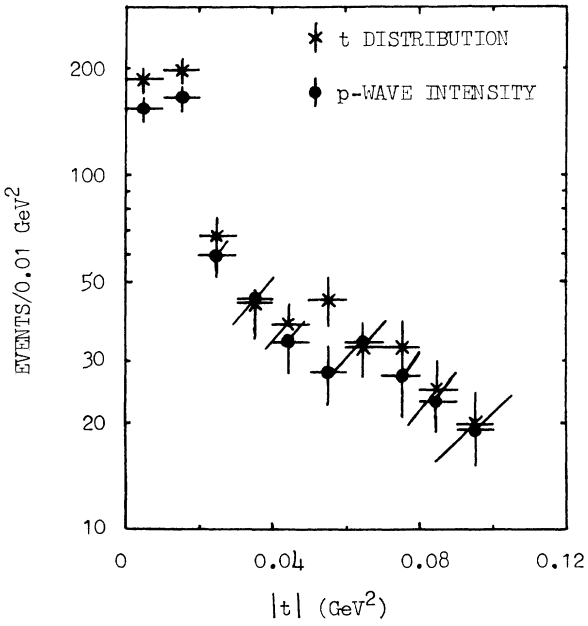

FIG. 13. The helicity-conserving p-wave intensity I_p and t distributions.

to the high intensity of the e^+e^- pair background, and due to events having very small projected opening angles and could not be distinguished from the e^+e^- pairs.

A. Pair-production cross section

Knasel[24] evaluated, numerically precise to ±0.5%, the e^+e^- pair-production cross section, after applying various corrections to the theoretical results of Jost, Luttinger, and Slotnick.[25] From Knasel's data we have used an average value of 20.1± 0.1 mb for the total pair-production cross section over the photon energy range of 4.7–6.2 GeV.

B. Differential cross section for $\gamma d \to \rho^0 d$

To the reaction $\gamma d \to \pi^+\pi^- d$ a total of 1176 two- and three-prong events fitted within a photon energy range of 4.7–6.2 GeV. To calculate the total cross section for ρ^0 production in this channel, we made the following three corrections:

1. Correction for scanning

(a) Due to small opening angles. We have applied the scanning correction for those events which has a very small projected opening angle between the pion tracks and could not be distinguished from e^+e^- pairs. Losses due to this were estimated by determining the deviation from the isotropy in the distribution of the angle between the optical axis direction and the projection of the vector $(\vec{\pi}^+ \times \vec{\pi}^-)$ onto the plane perpendicular to the beam direction. $\vec{\pi}$ is the three-momentum of the pion in the laboratory frame. The correction was (33±5)% for this reaction.

(b) Due to high e^+e^- pair background. Losses due to the high intensity of the e^+e^- pair background were estimated from the double-scan efficiencies of two- and three-prong events. This gave a correction of (8±1)% to the events.

2. Correction for unprocessed events

The unprocessed events consist of those events which are unmeasurable, poorly measured, and no-fit events (Table I). We have distributed among the different channels these two- and three-prong events in the same proportions as the fitted events. In case of ambiguity between 3C and 0C fits, the 3C fit was given a weighting factor of 1, whereas for n ambiguities amongst 3C fits the weighting factor was $1/n$ for each channel. This distribution gave a total correction of (11±1)% to the events.

3. Correction for photon energy selection

The e^+e^- pairs have been counted without imposing any selection criteria on the incoming photon energy. But the hadronic events are considered only within the fitted-photon-energy range of 4.7–6.2 GeV. To correct for the difference between the energy spectra of the pairs counted and that of ρ^0 events, we have used the photon energy spectra of Fig. 1. This correction was (18±3)%.

After putting in all these corrections the total ρ^0 photoproduction cross section in this channel comes out to be (9.1±0.8) μb. The error also includes uncertainty due to the background. This is in good agreement with the previously obtained values.[4]

C. Photoproduction of ω, ϕ, ρ', A_1 mesons

To investigate the production of ω, ϕ, ρ', and A_1 mesons in the final states $\pi^+\pi^-\pi^0 d$, $K^+K^- d$, $2\pi^+2\pi^- d$, and $\pi^+2\pi^- pp$, respectively, the following reactions were looked into:

$$\gamma d \to \pi^+\pi^-\pi^0 d, \tag{11}$$

$$\gamma d \to K^+K^- d, \tag{12}$$

$$\gamma d \to 2\pi^+2\pi^- d, \tag{13}$$

$$\gamma d \to \pi^+2\pi^- pp. \tag{14}$$

For further studies only those events wer considered which had fitted photon energy in the interval 4.7–6.2 GeV. No attempts were made to resolve the fit ambiguities of these channels with the other channels (Table II).

(a) Photoproduction of ω and ϕ mesons. There are not as many experiments on coherent ω and ϕ photoproduction as for ρ^0. These experiments are more difficult in that we are dealing with a much smaller cross section, and the decay modes are more fifficult to isolate. The only bubble-chamber data at 4.3 GeV on coherent ϕ photoproduction, $\gamma d \to \phi d$, have been published by Weizmann group[8] (1972) with rather large statistical uncertainties. The meson photoproduction on d at 6.2 and 8.25 GeV has been studied only at Cornell[26] using counters.

We attempted both hypotheses (11) and (12) for the three-prong events. For the two-prong events hypothesis (11) was not tried, because in this reaction the events with invisible d recoil have two unmeasured particles which are difficult to handle. The 3π and $2K$ mass distributions for the reactions (11) and (12), respectively, in Fig. 14 are for $-t < 0.15$ GeV^2 (momentum transfer from the target to the recoil deuteron). There are indications of ω and ϕ productions in these mass distributions, but the statistics are insufficient to make mass fits.

(b) Photoproduction of ρ' meson. There are several reasons to expect vector mesons to be heavier than the ϕ to exist. The existence of such particles would have a great impact on the vector-dominance model (VDM). It is of general interest, beyond the VDM, to search for such particles since the quark model and Veneziano model predict the existence of states at masses of ~1.25 GeV and between 1.5–1.6 GeV. Coherent photoproduction of such a meson, ρ', has been reported by Smadja *et al.*[27] from the reaction $\gamma p \to p 2\pi^+ 2\pi^-$ at 9.3 GeV. The 4π mass spectrum showed an enchancement near 1.6 GeV.

All four-and five-prong events were attempted for hypothesis (13). The 4π mass distribution is shown in Fig. 15. Owing to limited statistics we cannot draw any conclusion with respect to the existence of the ρ' meson.

(c) Photoproduction of the A_1 meson. On using pion beams in studying the A_1 meson, a $\rho\pi$ enhancement at 1.1 GeV, it was pointed out[28] that this could also be due to a Deck-type kinematic effect. One of the main reasons to perform our experiment was to study the channel $\gamma n \to \pi^+\pi^-\pi^- p$. It was suggested by Poe *et al.*[29] that in this channel the A_1 production would be free from the Deck effect.

We have tried all four- and five-prong events for hypothesis (14). The 3π mass distribution in Fig. 15 is for $-t < 0.15$ GeV^2, and only those events are plotted here for which at least one of the $\pi^+\pi^-$ mass combinations lies within the mass range of 0.6–0.85 GeV. In this mass distribution the A_2 peak is present, but there is no indication of A_1-meson production.

V. RESULTS AND CONCLUSIONS

We have found that the ρ^0 production in the $\gamma d \to \rho^0 d$ channel is shifted to lower masses than found in interactions using pion beams. We have also found that the ρ^0 shape is skewed with respect to a p-wave Breit-Wigner distribution, and changes shape as a function of t. The prediction of Ross and Stodolsky that the mass-skewing factor, $(M/M_{\pi\pi})^4$, should work at $t=0$ is not supported by the data near $t=0$.

We have been able to determine nine independent ρ^0 density-matrix elements because of the high degree of linear polarization of our photon beam. These parameters are given in Table IV and Fig. 9 for helicity, Gottfried-Jackson, and Adair frames. From these matrix elements we have been able to separate the contributions for ρ^0 production by natural- and unnatural-parity exchanges. It has been found that this reaction proceeds al-

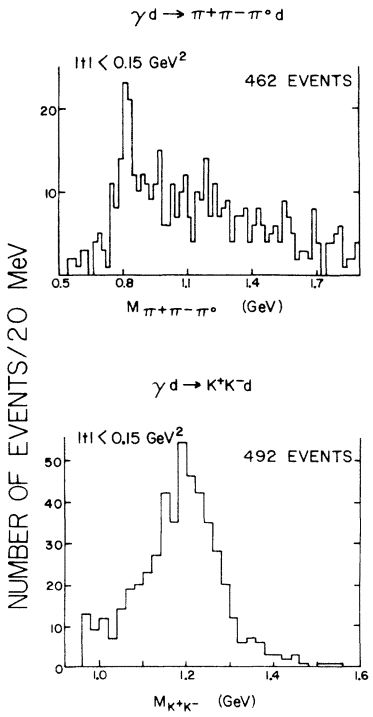

FIG. 14. 3π and K^+K^- mass distributions in the final states $\pi^+\pi^-\pi^0 d$ and $K^+K^- d$, respectively.

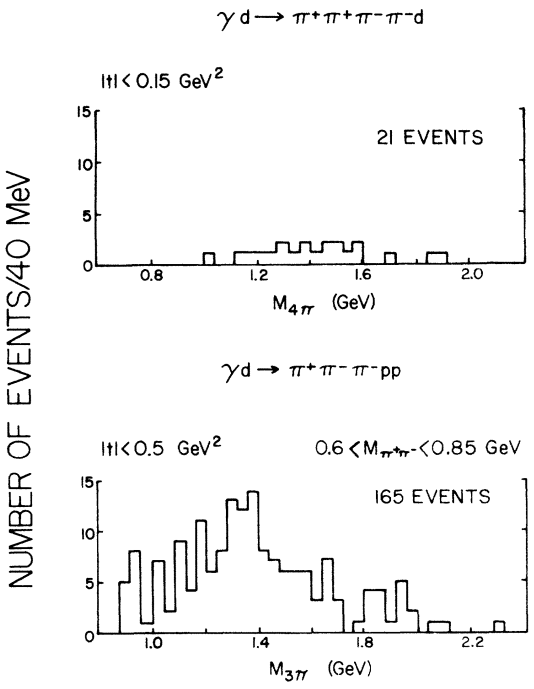

FIG. 15. 4π and 3π mass distributions in the final states $2\pi^+ 2\pi^- d$ and $\pi^+\pi^-\pi^- pp$, respectively.

most completely through the natural-parity exchange. The contributions from the unnatural-parity exchanges are only $(5.3\pm4.5)\%$, and the value of asymmetry ratio, Σ, is 1.1 ± 0.2 over the momentum transfer range of $|t| \leq 0.25$ GeV^2.

The production of the ρ^0 in this reaction has been found to conserve s-channel helicity up to $-t \approx 0.15$ GeV^2. We believe that these features may be general characteristics of diffractive processes.[30]

From the parameterized fitting to the data we find the ρ^0 mass and width as (766 ± 5) and (139 ± 11) MeV, respectively. The ρ^0 production cross section in this reaction channel at 5.5 GeV has been found to be (9.1 ± 0.8) μb.

ACKNOWLEDGMENTS

We wish to thank the SLAC operations crew of the accelerator and the 82-in. bubble-chamber operation group. In particular we thank J. Murray, R. Gearhart, and R. Watt for their support. We acknowledge the diligent work of our scanners at U. C., Riverside, and LBL. We also appreciate the assistance of Dr. T. L. Schalk in the early stages of the experiment.

---

*Work supported in part by U.S. Energy Research and Development Administration.

[1]J. J. Murray and P. R. Klein, SLAC Report No. TN-67-19, 1967 (unpublished).
[2]C. K. Sinclair *et al.*, IEEE Trans. Nucl. Sci. 16, 1065 (1969).
[3]R. A. Gearhart *et al.*, Nucl. Instrum. Meth. 75, 220 (1969).
[4]H. G. Hilpert *et al.*, Nucl. Phys. B21, 93 (1970); B23, 45 (1970).
[5]L. Criegee *et al.*, Phys. Lett. 28B, 282 (1968); Phys. Rev. Lett. 25, 1306 (1970).
[6]G. Diambrini-Palazzi *et al.*, Phys. Rev. Lett. 25, 478 (1970).
[7]SLAC-Berkeley-Tufts Collaboration, Phys. Rev. Lett. 24, 960 (1970); 24, 1469 (1970); K. C. Moffeit, LBL Report No. UCRL-19890, Ph.D. thesis, 1970 (unpublished).
[8]Y. Eisenberg *et al.*, Phys. Rev. Lett. 25, 764 (1970); Y. Eisenberg *et al.*, Nucl. Phys. B42, 349 (1972).
[9]G. Alexander *et al.*, Nucl. Phys. B68, 1 (1974).
[10]H. C. Albercht *et al.*, LBL Report No. UCRL-18528 Rev., 1968 (unpublished).
[11]Cambridge Bubble Chamber Group, Phys. Rev. 146, 994 (1966); Aachen-Berlin-Bonn-Hamburg-Heidelberg-München Collaboration *ibid.* 175, 1669 (1968).
[12]L. J. Lanzerotti *et al.*, Phys. Rev. 166, 1365 (1968); H. H. Bingham *et al.*, Phys. Rev. Lett. 24, 955 (1970); J. Ballam *et al.*, *ibid.* 24, 960 (1970).
[13]R. Vanderhagen *et al.*, Nucl. Phys. B13, 329 (1969); B. Werner *et al.*, Phys. Rev. 188, 2023 (1969).
[14]J. D. Jackson, Nuovo Cimento 34, 1644 (1964).
[15]M. Ross and L. Stodolsky, Phys. Rev. 149, 1172 (1966).
[16]P. H. Eberhard and W. O. Koellner, Computer Phys. Commun. 3, 296 (1972); 5, 163 (1973).
[17]R. L. Thews, Phys. Rev. 175, 1749 (1968).
[18]K. Schilling *et al.*, Nucl. Phys. B15, 397 (1970); B18, 332E (1970).
[19]V. P. Gupta, UCR Report No. UCR 34 P107B-180, Ph.D. thesis, 1974 (unpublished).
[20]N. Schmitz, *Proceedings of the 1965 Easter School for Physicists*, Report No. CERN 65-24, Vol. 1, 1965 (unpublished).
[21]Y. Eisenberg *et al.*, Phys. Lett. 22, 223 (1966).
[22]F. Cooper, Phys. Rev. 167, 1314 (1968).
[23]G. Cohen-Tannoudji *et al.*, Nuovo Cimento 55A, 412 (1968).
[24]T. M. Knasel, DESY Report No. 70/3, 1970 (unpublished).
[25]J. Jost, J. M. Luttinger, and M. Slotnick, Phys. Rev. 80, 189 (1950).
[26]G. McClellan *et al.*, Phys. Rev. Lett. 26, 1593 (1971).
[27]G. Smadja *et al.*, Phys. Lett. 41B, 635 (1972).
[28]S. D. Drell and K. Hiida, Phys. Rev. Lett. 7, 199 (1961); R. T. Deck, *ibid.* 13 (1964).
[29]R. T. Poe *et al.*, Phys. Rev. Lett. 22, 551 (1969).
[30]F. J. Gilman *et al.*, Phys. Lett. 31B, 387 (1970).